Journal of NUCLEAR SCIENCE and TECHNOLOGY, Vol. 39, No. 11, p. 1190–1198 (November 2002)

Applications of Artificial Neural Network for the Prediction of Flow Boiling Curves

Guanghui SU[1,2,*], Kenji FUKUDA[2], Koji MORITA[2], Mark PIDDUCK[2], Dounan JIA[1], Tatsuya MATSUMOTO[2] and Ryo AKASAKA[2]

[1]*Xi'an Jiaotong University, 710049, No. 28 Xianing West Road, Xi'an City, P.R. China*
[2]*Kyushu University, 6-10-1, Hakozaki, Higashi-ku, Fukuoka 812-8581*

(Received March 29, 2002 and accepted in revised form July 30, 2002)

An artificial neural network (ANN) was applied successfully to predict flow boiling curves. The databases used in the analysis are from the 1960's, including 1,305 data points which cover these parameter ranges: pressure P=100–1,000 kPa, mass flow rate G=40–500 kg/m^2·s, inlet subcooling ΔT_{sub}=0–35°C, wall superheat ΔT_w=10–300°C and heat flux Q=20–8,000 kW/m^2. The proposed methodology allows us to achieve accurate results, thus it is suitable for the processing of the boiling curve data. The effects of the main parameters on flow boiling curves were analyzed using the ANN. The heat flux increases with increasing inlet subcooling for all heat transfer modes. Mass flow rate has no significant effects on nucleate boiling curves. The transition boiling and film boiling heat fluxes will increase with an increase in the mass flow rate. Pressure plays a predominant role and improves heat transfer in all boiling regions except the film boiling region. There are slight differences between the steady and the transient boiling curves in all boiling regions except the nucleate region. The transient boiling curve lies below the corresponding steady boiling curve.

KEYWORDS: artificial neural network, boiling curve, pressure, mass flow rate, inlet subcooling, heat flux, heat transfer

I. Introduction

Flow boiling has been studied by many researchers in the last century and undoubtedly will continue to be studied in the future. One reason is because flow boiling has an extremely high heat transfer coefficient, it has been widely employed in energy conversion systems such as nuclear power reactor systems, chemical processes, oil systems, refrigeration systems and so on. Another reason is because there are many factors that have an influence on flow boiling. Hence, it is an extremely complex and illusive process.[1)] Boiling curves, which show qualitatively the dependence on the wall heat flux Q on the wall superheat ΔT_w (defined as the difference between the wall temperature T_w and the saturation temperature T_s of the fluid) are very important for evaluating the effectiveness of the emergency core cooling system of a water cooled nuclear reactor. Researchers such as Berenson,[2)] Spiegler,[3)] Bergles[4)] and others[5–12)] have all used boiling curves since Nukiyama[13)] presented the first boiling curve in 1934. In general, these boiling curves do not always include nucleate boiling, transition boiling and film boiling regions, as shown in **Fig. 1**. They often show just one or two of the three parts. For highly subcooled flow boiling, there is an additional region between transition and film boiling, the intermediate film boiling region, where the heat flux is nearly independent of the wall superheat. Thus none of these boiling curves may be used as a database in the analysis of nuclear reactor thermohydraulics and/or safety. We have to use the correlations such as Jens-Lottes,[14)] Thom,[15)] Rohsenow[16)] or Chen[17)] for nucleate boiling, Tong,[18)] Milich,[19)] King[20)] or Berenson[21)] for transition boiling and Groeneveld[22)] or Bromley[23)] for film boiling to calculate the heat transfer coefficient. In the calculation process, the different correlations will be used in different heat transfer regions. The heat transfer coefficient is discontinuous when one carries out the reactor thermohydraulic and safety analyses in all flow boiling regions, therefore the correlation must be changed according to heat transfer modes. So far, complete theoretical correlations have not been developed to predict the boiling heat flux or heat transfer coefficient in all boiling regions specifically as a function of wall superheat.[11)] To solve this problem, the authors trained an artificial neural network (ANN) using the data of the past four decades that have been tabulated in **Table 1**. The ANN can be used to predict a complete boiling curve. The heat flux, as a function of wall superheat, may be obtained using the ANN.

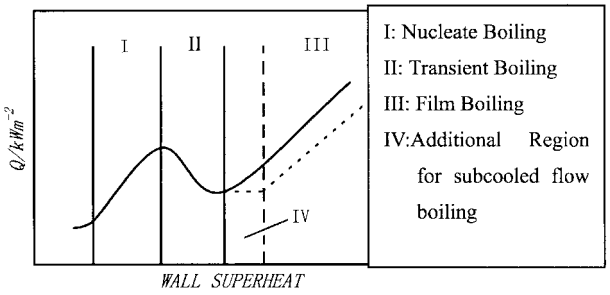

Fig. 1 Schematic diagram for flow boiling curves

II. Artificial Neural Network (ANN)

The ANN consists of a layer of input neurons, a layer of output neurons and one or more hidden layers which are made up of many interconnected simple nonlinear neurons. Exter-

*Corresponding author, Tel.&Fax. +81-92-642-3789, +86-29-266-7082,
E-mail: sugh@nucl.kyushu-u.ac.jp, ghsu@mail.xjtu.edu.cn

Table 1 Database of flow boiling

Ref. No.	Test section	Boiling medium	Variable factors	Type of boiling
6)	Stainless steel and Inconel; Circular duct (tube); D_O=19.1 and 15.9 δ=1.65, 0.89 and 1.02 L=4, 3.5	Water	P=0.1, G=100–400, ΔT_{sub}=10–80, T_w=270–800	BC and CD
8)	D_O=13.1 and δ=0.559 for Zircaloy; D_O=14.0 and δ=0.635 for Al; D_O=12.7 and δ=0.38 for Inconel; D_O=12.7 and δ=0.38 for Cu; Tube	Water	P=0.1, G=68–203, ΔT_{sub}=0–28,	BC and CD
9)	D_O=16.1, δ=0.8, L=3.66; Tube	Water	P=0.1–0.4, G=25–75, ΔT_{sub}=33–81	BC and CD
10)	Monel; D_O=10, δ=0.15, L=0.05; Tube	Water and N_2	P=0.1–1.0, G=25–500, ΔT_{sub}=5–50	BC and CD
24)	Correlation	Water		BC and CD
25)	D_O=12.7; Tube	Water	P=0.1, G=34–102, ΔT_{sub}=0–28	CD
26)	Ni; D_O=32, δ=5.575, L=0.05; Tube	Water	P=0.1–1.0, G=100–200, ΔT_{sub}=30	BC and CD
27)	Correlation			CD
28)	Cu; D_O=32, δ=11, L=0.05; Tube	Water	P=0.1–1.2, G=25–500, ΔT_{sub}=3–30	BC
29)	Correlation	Water		BC and CD
30)	Cu; D_O=95.3, δ=41.3, L=0.0572; Tube	Water	P=0.1, G=136, ΔT_{sub}=0	BC and CD
31)	Cu, D_O=95.3, δ=41.3, L=0.0572; Tube	Water	P=0.1, G=68–203, ΔT_{sub}=0–28	BC, CD and DE
32)	Cu, D_O=95.3, δ=41.3, L=0.0572; Tube	Water	P=0.1, G=136, ΔT_{sub}=0–28	BC and CD
33)	Correlation	Water		BC and CD

(Note) D_O: Tube outside diameter (mm), δ: Tube wall thickness (mm), L: Tube length (m), P: Pressure (MPa), G: Mass flow rate (kg/m^2·s), ΔT_{sub}: Inlet subcooling (°C), T_w: Initial wall temperature (°C). BC: Nucleate boiling, CD: Transition boiling, DE: Film boiling

nal data enter the ANN through the input nodes. The output data are obtained from the output nodes after nonlinear transformations. The ANN is characterized by the network structure: the weights by which the network will learn to associate a given output with a given input, neural activation properties and the learning rules which modify the weights of neurons. The weight adaptation algorithm which we adopted in this paper was the Back-Propagation (BP) algorithm.

A net input v_j to a neuron in a hidden layer k is calculated by the formula

$$v_j = \sum_{i=1}^{n} w_{ji} o_i + \theta_j, \tag{1}$$

where n is the number of $k-1$ layer neurons, the weights are denoted by w_{ji}, and the threshold offset by θ_j.

The output of the neuron o_j is given by an activation function. Many different activation functions are in common use, such as sigmoid, hyperbolic tangent, *etc.* The function adopted for the present study was

$$o_j = 1/(1 + \exp(-v_j)). \tag{2}$$

Signal processing of the unit neuron is shown in **Fig. 2**.

The procedure for training the weights w_{ji} is to improve the weights in order to reduce the average system error E_{AV}

$$E_{AV} = \frac{1}{2N} \sum_{n=1}^{N} \sum_{j} (d_j(n) - o_j(n))^2, \tag{3}$$

where $d_j(n)$ is the desired output. Improved values of the

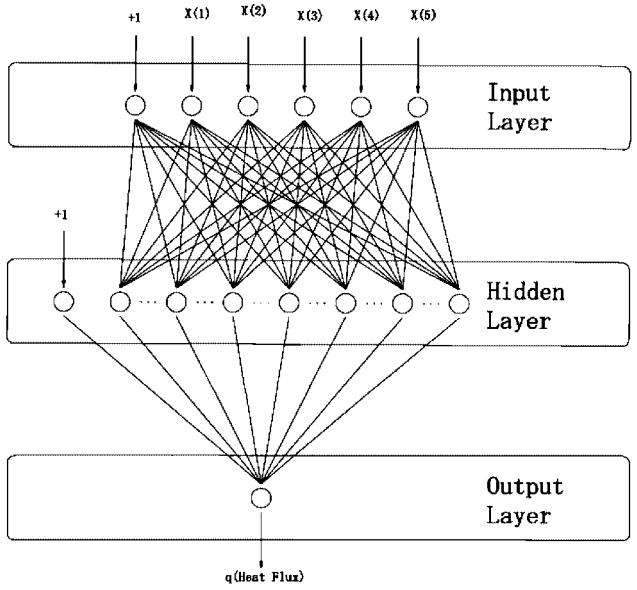

Fig. 2 Artificial neural network

weights can be achieved by taking incremental changes Δw_{ji} proportional to $\partial E_{AV}/\partial w_{ji}$, that is

$$\Delta w_{ji} = -\eta(\partial E_{AV}/\partial w_{ji}), \tag{4}$$

where η is the learning rate which has typical values lying between 0.001 and 1.0. From this, the new weights for step $m+1$ are given as

$$w_{ji}(m+1) = \alpha w_{ji}(m) + \eta\delta_j o_i, \tag{5}$$

where a momentum coefficient or an acceleration parameter denoted by α is used to improve the training time and δ_j is given by

$$\delta_k = (d_k - o_k)o_k(1 - o_k) \tag{6}$$

for output neurons and

$$\delta_j = o_j(1 - o_j)\sum_k \delta_k w_{kj} \tag{7}$$

for hidden neurons.

Figure 3 shows the signal flow chart and **Fig. 4** shows the N-S chart of the calculating code. Artificial neural networks have the advantage that a formal model structure to fit the experimental data is not required. The role of the ANN is to predict parameters required by the analytical correlation. However these parameters were instead set to a constant value obtained by the usual best-fitting techniques. The proposed methodology is expected to allow us to achieve accurate results in boiling curve data processing. The databases, as listed in Table 1, are experimental data from the 1960's. They contain 1,305 data points that cover the following parameter ranges:

Pressure P: 100–1,000 kPa
Mass flow rate G: 40–500 kg/m^2·s
Inlet subcooling ΔT_{sub}: 0–35°C
Wall superheat ΔT_w: 10–300°C
Heat flux Q: 20–8,000 kW/m^2.

Cybenko[34] reported that ANN's with two hidden layers are sufficient for S-type activation functions (sigmoid and hyperbolic tangent functions). However, one hidden layer is enough for a small ANN. Lippman[35,36] reported that the maximum node number of the hidden layer K equals $(M+1)N$, where M is the node number of the input layer and N is that of the output layer.

The initial weights heavily affect the performance of the BP ANN. Thus the problem is to use an algorithm which will allow the ANN to work properly and yield the final weights to achieve accurate results. Wilde[37] suggested that the training of the ANN could begin by making a random guess for the weights. Do not allow zero as a guess for a weight as it may stay stuck at zero during the back-propagation procedure. The parameters describing the boiling conditions which were provided to the ANN as the inputs are shown in **Table 2**. It was found that the input signals do not share the same importance regarding the ANN accuracy and that the most important parameter was the wall superheat ΔT_w.

III. Prediction of Flow Boiling Curves by ANN

An ANN was trained for predicting flow boiling curves based on the databases shown in Table 1. The input parameters are listed in Table 2. The output is the heat flux in kW/m^2. One can obtain the results conveniently if one inputs the required parameters into the ANN. For example, if P=0.2 MPa, ΔT_{sub}=15°C and G=200 kg/m^2·s are the input conditions, the steady and transient boiling curves can be obtained by the ANN as shown in **Fig. 5**. **Figure 6** shows the results obtained by the ANN. The experimental data and Lee's[24] correlation data were also plotted in Fig. 6. The agreement between experimental data and the ANN results are quite satisfactory. **Figure 7** shows the comparison between the heat fluxes obtained by the ANN and by experiments. The accuracy is ±30%. There are 1,305 data points in the database, of which 1,010 data points are inside the error band of ±30% and 295 data points are outside. The relative error E is defined as

$$E = \frac{Q_{\mathrm{ANN}} - Q_{\mathrm{EXP}}}{Q_{\mathrm{EXP}}} \times 100\%, \tag{8}$$

where Q_{ANN} is the heat flux predicted by the ANN and Q_{EXP} is that obtained by experiments.

The average error E_{AVG} is 24.86%, which is defined as

$$E_{AVG} = \frac{1}{N}\sum_{i=1}^{N} |E|_i, \tag{9}$$

where N=1,305.

The root-mean-square error RMS is 42.33%, which is defined as

$$RMS = \sqrt{\frac{1}{N}\sum_{i=1}^{N} E_i^2}. \tag{10}$$

Figure 8 shows the effects of inlet subcooling on the boiling curves. Cheng's data were also plotted in Fig. 8 in order to verify the ANN. In general, for all heat transfer modes encountered, the heat flux increases with increasing inlet subcooling. This conclusion agrees with that of Chen,[6] Cheng[30] and Ragheb.[25] However, in the film boiling and nucleate boil-

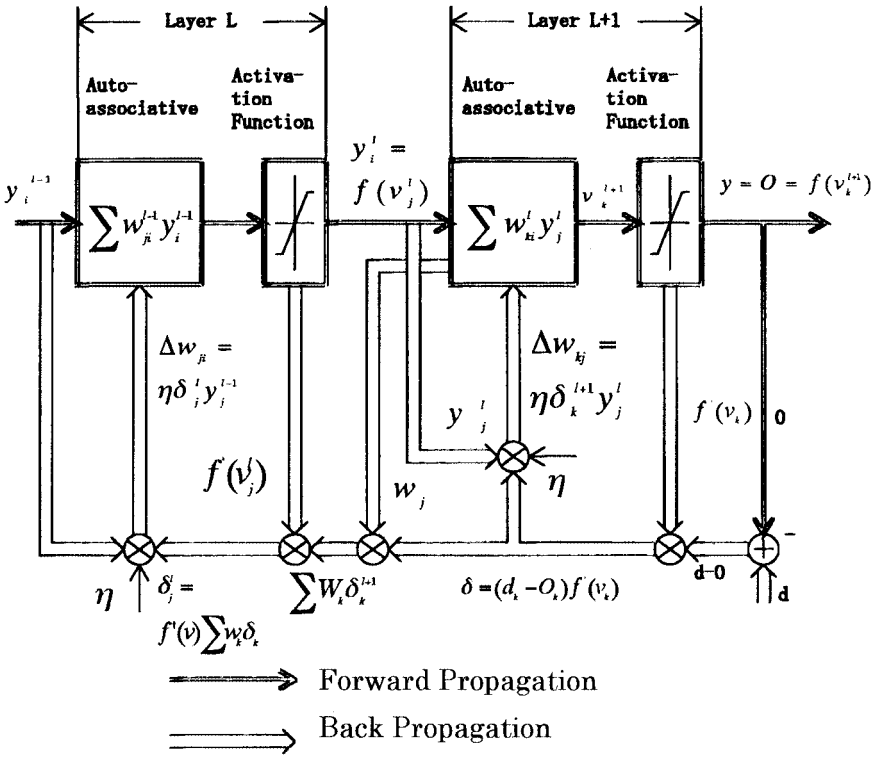

Fig. 3 Signal flow chart (layout)

Table 2 Input parameters of ANN for flow boiling

Input nodes	X(1)	X(2)	X(3)	X(4)	X(5)
Parameters	Pressure in kPa	Mass flow rate in kg/m^2·s	Inlet subcooling in °C	Wall superheat in °C	Steady-state or transient state

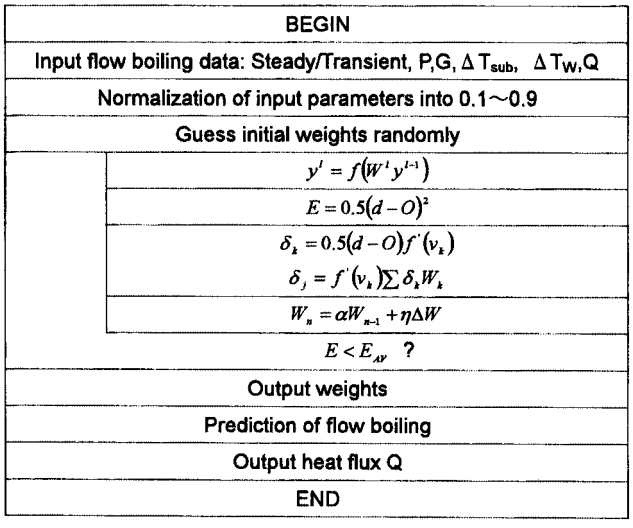

Fig. 4 N-S flow chart (layout)

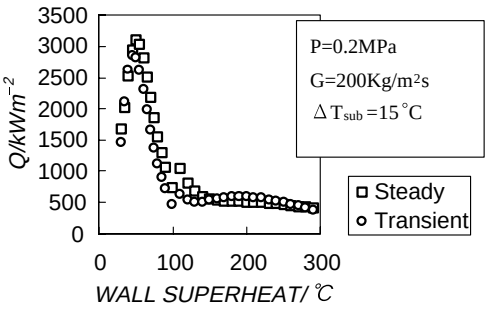

Fig. 5 Boiling curves obtained by ANN

ing regions, this effect is very small. Therefore, the effect of inlet subcooling on boiling curves can be neglected in the nucleate and film boiling regions. Jens and Lottes[14] presented a correlation for nucleate boiling when pressure is in the range 0.7 MPa$\leq P \leq$17.2 MPa as follows:

$$\Delta T_W = 25\left(\frac{Q}{10^6}\right)^{0.25} \exp\left(\frac{-P}{6.2}\right), \tag{11}$$

where $\Delta T_W = T_W - T_S$; T_W is the wall temperature and T_S is the saturated temperature of fluids.

Thom[15] also presented a correlation for nucleate boiling when pressure is in the range 5.17 MPa$\leq P \leq$13.79 MPa as follows:

$$\Delta T_W = 0.0225 Q^{0.5} \exp\left(\frac{-P}{8.69}\right). \tag{12}$$

These correlations show that the heat flux in the nucleate boil-

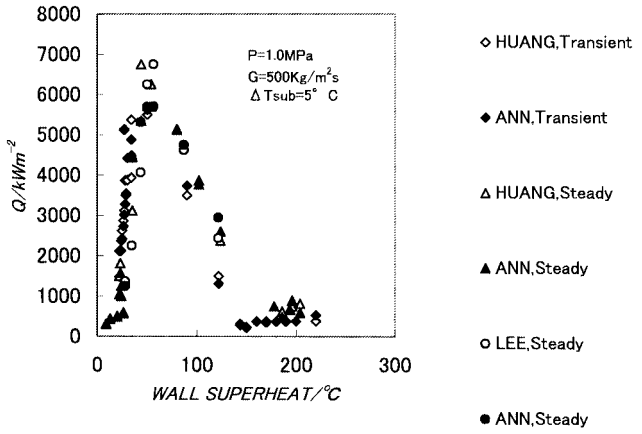

Fig. 6 Comparison between the results obtained by ANN and experiments (I)

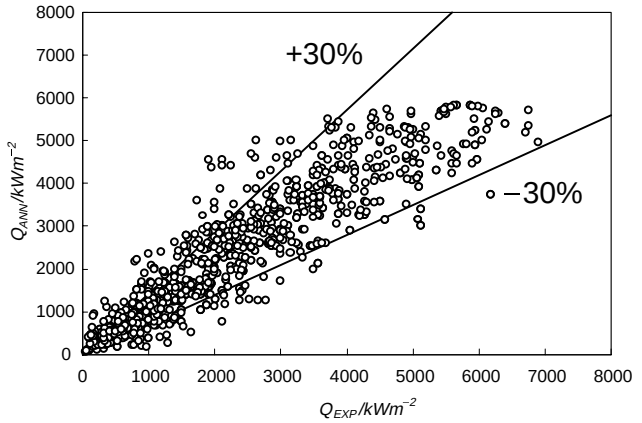

Fig. 7 Comparison between the results obtained by ANN and experiments (II)

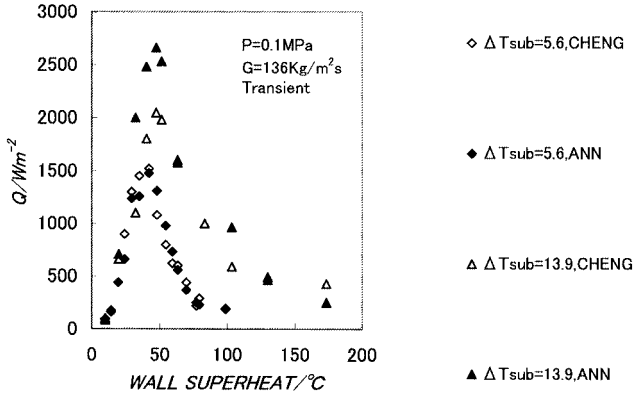

Fig. 8 The effect of inlet subcooling on boiling curves (I)

ing region is only related to the pressure and the wall superheat. The results obtained by the ANN show that the inlet subcooling effect on nucleate boiling is sufficiently small and that one can neglect it.

However, **Fig. 9** shows that the influences of inlet subcooling are very small for all boiling regions except critical heat flux (CHF). The same trends were found in Huang's experimental data.[10] It should be emphasized that inlet subcooling has significant effect on CHF as shown in Fig. 9.

Figure 10 shows the effect of mass flow rate on boiling curves. It indicates that the mass flow rate has no significant effect on nucleate boiling curves. As mentioned above, the Jens-Lottes and the Thom correlations give the same conclusion. The transition boiling and the film boiling heat fluxes will increase with an increase of mass flow rate. However, the effect of mass flow rate on the film boiling curve is less than that on the transition boiling curve. An increase of mass flow rate improves the heat transfer in the transition boiling region, obviously due to the more efficient vapor transport ability and increased flow turbulence.

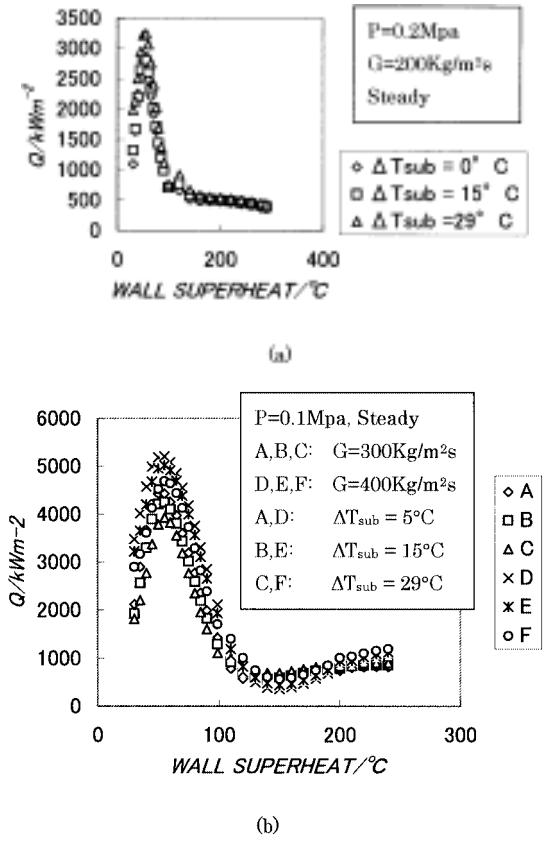

Fig. 9 The effects of inlet subcooling on boiling curves (II)

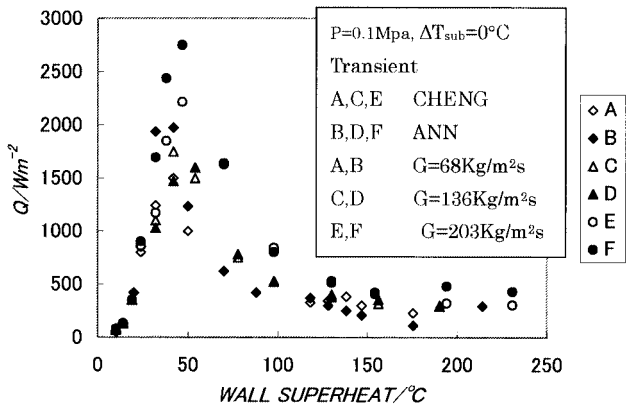

Fig. 10 Effect of mass flow rate on boiling curves

Pressure plays a predominant role and improves heat transfer in all boiling regions except the film boiling region. **Figure 11** shows the effect of pressure on boiling curves. In this figure, the results obtained by the ANN were compared with those of selected references.[10,24,38] The ANN results agree well with the references' data. An increase in pressure clearly improves the heat transfer in nucleate and transition boiling regions. In the nucleate boiling region, pressure is the only parameter which has an effect on the boiling curve in the Jens-Lottes and Thom correlations. However, the influence of pressure on the film boiling curve is less than that on other boiling modes. Shiotsu's experimental data[39] also demonstrated the minimal effect of pressure on film boiling.

Figure 12 shows the comparison between the steady boiling curve and the transient curve obtained by the ANN. Figure 12(a) was plotted under the conditions of P=0.1 MPa, G=200 kg/m^2·s and ΔT_{sub}=5°C. For Fig. 12(b), P=0.4 MPa, G=200 kg/m^2·s and ΔT_{sub}=5°C. Figures 12(a) and (b) show that there are no obvious differences between the steady and the transient boiling curves. Figure 12(c) under the conditions P=0.8 MPa, G=500 kg/m^2·s and ΔT_{sub}=29°C shows that there is a slight difference between them in all boiling regions except in the nucleate boiling region. The parameters of pressure P, mass flow rate G and

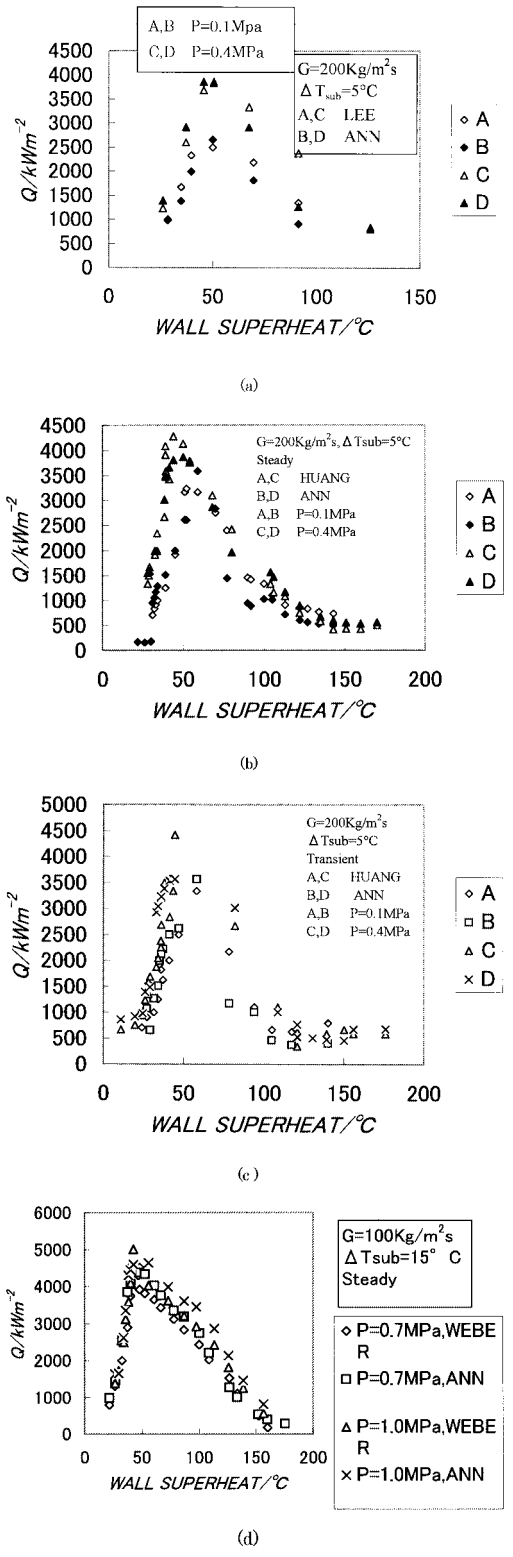

Fig. 11 The effects of pressure on boiling curves

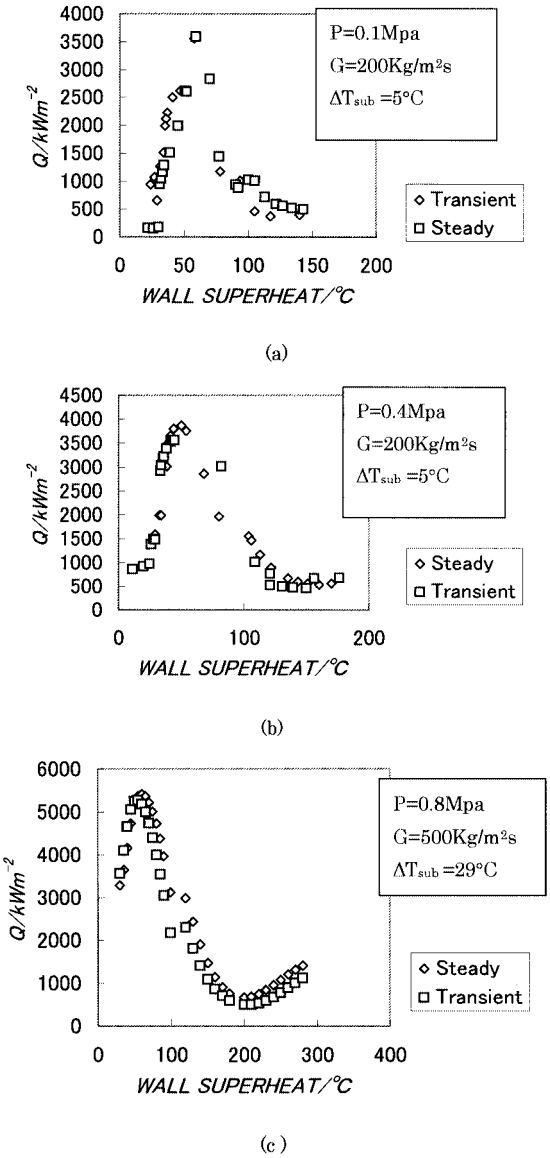

Fig. 12 The comparison between steady boiling curve and transient one

inlet subcooling ΔT_{sub} in Fig. 12(c) are higher than those of Figs. 12(a) and (b). Thus the differences between the steady and the transient boiling curves are influenced by such parameters as pressure P, mass flow rate G and inlet subcooling ΔT_{sub}. Figure 12(c) also shows that the transient boiling curve lies below the corresponding steady one. Huang[10] reported that there is no significant difference between the transient and the steady boiling curves in all boiling regimes for the parameter ranges of $P<0.7$ MPa, $G<300$ kg/m^2·s and $\Delta T_{sub}<15$°C. Beyond these ranges, however, the difference becomes obvious in the transition boiling regime. Good agreement between the results obtained by the ANN and Huang's report was found.

As mentioned above, all of the parameters (pressure P, mass flow rate G and inlet subcooling ΔT_{sub}) can influence the transition boiling curve. Thus we can say that transition boiling is a complex physical phenomenon. It involves unsteady processes in the liquid and vapor phases of the test fluid, in the wall and at the boundaries of these media. Indeed, it is an intermediate heat transfer mode where the surface temperature is too high to maintain stable nucleate boiling but too low to maintain stable film boiling. Tong[40] called transition boiling "partial film boiling." A great number of parameters have an effect on transition boiling curves. Kalinin[41] reported that the following factors can affect transition boiling curves: parameters of the test section (shape, size, and roughness of the heat surface), thermophysical properties of material, boiling medium properties (hydrodynamic, thermodynamic, thermophysical), process conditions, characteristics of the force fields and the test section orientation relative to these fields, free or finite liquid volume velocity of the channel liquid or external flow past a test section. Although satisfactory results were obtained in our present paper, further studies are needed in order to improve the method of predicting boiling curves, especially of transition boiling curves, since only the parameters listed in Table 2 were selected as the input parameters to train the ANN.

IV. Discussions

It is well known that the heat transfer experimental data can be presented only in two different approaches following traditional research methods: representing the experimental data with the most compact set of equations although they may be empirical or semi-empirical or presenting them as boiling curves. Empirical or semi-empirical correlations are always the best-fit relationships of some experimental data with reasonable simplifying assumptions. They are limited in their range of application depending on the limitations of the experimental data. It is very difficult to theoretically perform a perfect correlation for all regions of heat transfer even though researchers can get the experimental data over a wide range. Boiling curves may be used to directly express the heat transfer under some conditions. However, it is inconvenient and difficult if the boiling curves are applied for the analytical codes of nuclear power systems. Therefore it is highly desirable to have some models that have the advantages of the above two approaches and may overcome their disadvantages.

Artificial neural network may be one of these models. The ANN is a simplified mathematical model of a biological neural network. It has the ability to learn directly from the experimental data. The ability to learn is one of the distinguishing features of the ANN. The ANN, a physiconeural model which may be inserted into the analytical codes, is used to predict the outputs as a function of input parameters after training according to the experimental data without the benefit of a best-fit analysis. All of these characteristics prompted the researchers to try to apply it for the study of heat transfer. The ANN has very recently become a topic of academic research of heat transfer and is still developing, especially for simulating the complex physical processes such as flow boiling heat transfer. Thibault[42] evaluated the potential of the ANN for correlating heat transfer data using three different examples: a thermocouple lookup table, a series of correlations between Nusselt and Rayleigh numbers for free convection around horizontal smooth cylinders and the problem of natural convection along slender vertical cylinders with variable surface heat flux. This paper clearly demonstrated that the ANN methodology may be used efficiently to model and correlate heat transfer data. Mahajan[43] and Su[44] presented their ANN models which can be used to predict the pool boiling curves. Mahajan trained a simple ANN for predicting the boiling curves of FC-70. The ANN has two input parameters, $\log Q$ and process index i, where $i=1$ for heating and $i=0$ for cooling and one output, $\log \Delta T$. However, Mahajian presented only one figure in which the ANN model and experimental boiling curve were compared. Su's ANN has seven input parameters, wall superheat, surface roughness, surface inclination, steady-state or transient heating or cooling, subcooling, pressure and type of boiling fluid and one output parameter, heat flux. The ANN can be used for predicting the pool boiling curves of water, *n*-pentane and methanol. Jambunathan[45] successfully applied the ANN for deducing convective heat transfer coefficients from experimental data. Mazzola[46] pointed out that the ANN was likely to be suitable for thermalhydraulic and heat transfer data processing. Su[47,48] reported that the ANN is a powerful and useful tool for correlating pool and flow boiling heat transfer data. However their databases of flow boiling were very limited. Indeed, a large quantity of experimental data for flow boiling heat transfer has been presented up to now. Therefore, the ANN can be used as a predictor of flow boiling heat transfer based on a state-of-the-art database without knowing the best-fit correlations due to the ANN's black-box characteristic. The predicted results can be obtained using the ANN if the required parameters are inputted after the ANN training. The researchers must strive to collect all the experimental data in order to train a perfect ANN in which all parameters that have effects on flow boiling will be considered within a wide parameter range. However the different experiments have been done under different conditions. As described in the last section, a number of parameters affect flow boiling heat transfer. Therefore, it is very difficult to train a perfect ANN which can be suitable for different databases in one step. The present study demonstrates that the ANN can be used to simulate the flow boiling behaviors appropriately based on the known experimental data. Further work is in progress to exploit an universal ANN using non-dimensionalized param-

eters to overcome the difficulty of uniting the input parameters.

V. Conclusions

An artificial neural network (ANN) was applied successfully to predict flow boiling curves. The ANN was trained to predict flow boiling curves with a database composed of experimental data from the 1960's. It included 1,305 data points that cover the following parameter ranges: pressure P=100–1,000 kPa, mass flow rate G=40–500 kg/m^2·s, inlet subcooling ΔT_{sub}=0–35°C, wall superheat ΔT_w=10–300°C and heat flux Q=20–8,000 kW/m^2. The proposed methodology allows accurate results to be achieved, thus the ANN is suitable for boiling curve data processing.

The effects of the main parameters such as inlet subcooling, mass flow rate, pressure, and steady/transient state on flow boiling curves were analyzed and the following results were obtained.

(1) Heat flux increases with increasing inlet subcooling in the transition boiling regions. However, the effects of inlet subcooling on boiling curves can be neglected in the nucleate and film boiling regions.

(2) Mass flow rate has no significant effect on nucleate boiling curves. The transition boiling and the film boiling heat fluxes will increase with an increase in the mass flow rate. The effects of mass flow rate on film boiling curves are less than those on transition boiling curves.

(3) Pressure plays a predominant role and improves heat transfer in all boiling regions except film boiling. An increase in pressure clearly improves the heat transfer in nucleate and transition boiling regions. The influence of pressure on film boiling curves is less than on other boiling modes.

(4) There are slight differences between the steady and the transient boiling curves in all boiling regions except the nucleate boiling region. The differences between them are influenced by such parameters as pressure, mass flow rate, inlet subcooling, *etc*. The differences will become significant if these main parameters are greater in value. The transient boiling curve lies below the corresponding steady boiling curve.

References

1) V. K. Dhir, "Nucleate and transition boiling heat transfer under pool and external flow conditions," *Int. J. Heat Fluid Flow*, **12**, 290–314 (1991).
2) P. J. Berenson, "Experiments on pool-boiling heat transfer," *Int. J. Heat Mass Transfer.*, **5**, 985–999 (1962).
3) P. Spiegler, J. Hopenfeld, M. Silberberg, Jr., C. F. Bumpus, A. Norman, "Onset of stable film boiling and the foam limit," *Int. J. Heat Mass Transfer.*, **6**, 987–994 (1963).
4) A. E. Bergles, W. G., JR Thompson, "The relationship of quench data to steady-state pool boiling data," *Int. J. Heat Mass Transfer*, **13**, 55–68 (1970).
5) D. C. Groeneveld, S. R. M. Gardiner, "A method of obtaining flow film boiling data for subcooled water," *Int. J. Heat Mass Transfer*, **21**, 664–665 (1978).
6) W. J. Chen, Y. Lee, D. C. Groeneveld, "Measurement of boiling curves during rewetting of a hot circular duct," *Int. J. Heat Mass Transfer*, **22**, 973–976 (1979).
7) K. Makino, I. Michiyoshi, "Effects of the initial size of water droplet on its evaporation on heated surfaces," *Int. J. Heat Mass Transfer*, **22**, 979–981 (1979).
8) H. S. Ragheb, S. C. Cheng, D. C. Groeneveld, "Observations in transition boiling of subcooled water under forced convective conditions," *Int. J. Heat Mass Transfer*, **24**, 1127–1137 (1981).
9) S. T. Wang, R. A. Seban, "Heat transfer during the quench process that occurs in the reflood of a single vertical tube," *Int. J. Heat Mass Transfer*, **31**, 1189–1198 (1988).
10) X. C. Huang, G. Bartsch, D. Schroeder-richter, "Quenching experiments with a circular test section of medium thermal capacity under forced convection of water," *Int. J. Heat Mass Transfer*, **37**, 803–818 (1994).
11) V. K. Dhir, "Boiling heat transfer," *Annu. Rev. Fluid Mech.*, **30**, 365–401 (1998).
12) S. S. Hsieh, T. Y. Yang, "Nucleate pool boiling from coated and spirally wrapped tubes in saturated R-134a and R-600a at low and moderate heat flux," *J. Heat Transfer*, **123**, 257–270 (2001).
13) S. Nukiyama, "The maximum and minimum values of the heat Q transmitted from metal to boiling water under atmospheric pressure," *J. JSME*, **37**, 367–374 (1934).
14) W. H. Jens, P. A. Lottes, *Analysis of Heat Transfer, Burnout, Pressure Drop, and Density Data for High Pressure Water*," ANL-4627, Argonne National Lab., (1951).
15) J. R. S. Thom, W. M. Walker, T. A. Fallon, G. F. S. Reising, "Boiling in subcooled water during flow up heated tubes or annuli," *Proc. Institute of Mechanical Engineers*, 180 (Part 3C), (1966).
16) W. M. Rohsenow, "A method of correlating heat transfer data for surface boiling of liquids," *Trans. ASME*, **74**, 969–976 (1952).
17) J. C. Chen, *A Proposed Mechanism and Method of Correlation for Convective Boiling Heat Transfer with Liquid Metals*, BNL-7319, Brookhaven National Lab., (1966).
18) L. S. Tong, "Heat transfer in water-cooled nuclear reactors," *Nucl. Eng. Des.*, **6**, 301 (1967).
19) J. G. Collier, *Convective Boiling and Condensation*, McGraw-Hill Int. Book, New York, (1981).
20) S. Karl, *Heat Transfer in Condensation and Boiling*, Springer-Verlag, New York, (1992).
21) P. J. Berenson, "Transition boiling heat transfer," *4th Natl. Heat Transfer Conf.*, AIChE preprint 18, Buffalo, New York, (1960).
22) D. C. Groeneveld, *The Thermal Behavior of a Heated Surface at and beyond Dryout*, AECL-4309, Chalk River, Canada, (1972).
23) L. A. Bromley, N. LeRoy, J. A. Robbers, "Heat transfer in forced convection film boiling," *Ind. Eng. Chem.*, **45**, 2639–2646 (1953).
24) K. W. Lee, S. Y. Lee, "An investigation of transition boiling mechanisms of subcooled water under forced convective conditions," *Nucl. Eng. Des.*, **177**, 25–39 (1997).
25) H. S. Ragheb, S. C. Cheng, "Surface wetted area during transition boiling in forced convective flow," *J. Heat Transfer*, **101**, 381–383 (1979).
26) X. C. Huang, G. Bartsch, "About the second-order instability on an electrically heat temperature-controlled test section under forced convective boiling conditions," *Int. J. Heat Mass Transfer*, **36**, 2601–2612 (1993).
27) C. Pan, J. Y. Hwang, T. L. Lin, "The mechanism of heat transfer in transition boiling," *Int. J. Heat Mass Transfer*, **32**, 1337–1349 (1989).
28) X. C. Huang, P. Weber, G. Bartsch, "Comparison of transient

and steady-state boiling curves for forced upflow of water in a circular tube at medium pressure," *Int. Commun. Heat Mass Transfer*, **20**, 383–392 (1993).
29) S. C. Cheng, K. T. Heng, "A technique to construct a boiling curve from quenching data," *Lett. Heat Mass Transfer*, **3**, 413–420 (1976).
30) S. C. Cheng, K. T. Heng, W. Ng, "A technique to construct a boiling curve from quenching data considering heat loss," *Int. J. Multiphase Flow*, **3**, 495–499 (1977).
31) S. C. Cheng, W. W. L. Ng, K. T. Heng, "Measurements of boiling curves of subcooled water under forced convective conditions," *Int. J. Heat Mass Transfer*, **21**, 1385–1392 (1978).
32) S. C. Cheng, W. W. L. Ng, K. T. Heng, D. C. Groeneveld, "Measurements of transition boiling data for water under forced convective conditions," *J. Heat Transfer*, **100**, 382–384 (1978).
33) M. Dostie, Y. Mercadier, "A general correlation factor for the use of saturated boiling correlations in computing convective subcooling boiling heat transfer," *Proc. 8th Int. Heat Transfer Conf.*, San Francisco, CA, USA, Ed. by C. L. Tien, V. P. Carey, J. K. Ferrell, Vol. 5, 2155–2160 (1986).
34) G. Cybenko, "Continuous valued neural networks with two hidden layers are sufficient," Department of Computer Science, Tufts. University, Medford, MA., USA, (1988).
35) R. P. Lippmann, "An introduction to computing with neural nets," *IEEE ASSP Magazine*, Apr. 4–22 (1987).
36) R. P. Lippmann, "Pattern classification using neural networks," *IEEE Commun. Magazine*, Apr. 47–64 (1989).
37) P. D. Wilde, *Neural Network Models, Theory and Projects*, 2nd Ed., Springer (London), p. 37 (1997).
38) P. Weber, K. Johannsen, "Convective transition boiling of water at medium pressure," *Proc. 8th Int. Heat Transfer Conf.*, San Francisco, CA, USA, Vol. 5, (1990).
39) M. Shiotsu, K. Hama, "Film boiling heat transfer from a vertical cylinder in forced flow of liquids under saturated and subcooled conditions at pressures," *Nucl. Eng. Des.*, **200**, 23–38 (2000).
40) L. S. Tong, Y. S. Tang, *Boiling Heat Transfer and Two-phase Flow*, Taylor & Francis, Washington, D.C., p. 2 (1997).
41) E. K. Kalinin, I. I. Berlin, V. V. Kostiouk, "Transition boiling heat transfer," *Adv. Heat Transfer*, **18**, 241–323 (1987).
42) J. Thibault, B. P. A. Grandjean, "A neural network methodology for heat transfer data analysis," *Int. J. Heat Mass Transfer*, **34**[8], 2063–2070 (1991).
43) R. L. Mahajan, X. A. Wang, "Neural network models for thermally based microelectronic manufacturing processes," *J. Electrochem. Soc.*, **140**(8), 2287–2293 (1993).
44) G. H. Su, K. Fukuda, K. Morita, "Applications of artificial neural network for the prediction of pool boiling curves," *Proc. 10th Int. Conf. on Nuclear Engineering*, Arlington, VA, USA, Apr. 14–18, 2002, ICONE10-22487, copyright by ASME, (2002).
45) K. Jambunathan, S. L. Hartle, S. Ashforth-frost, V. N. Fontama, "Evaluating convective heat transfer coefficients using neural networks," *Int. J. Heat Mass Transfer*, **39**[11], 2329–2332 (1996).
46) A. Mazzola, "Integrating artificial neural networks and empirical correlations for the prediction of water-subcooled critical heat flux," *Rev. Gen. Therm.*, **36**, 799–806 (1997).
47) G. H. Su, K. Fukuda, "New methods of studying nuclear reactor thermohydraulics," *Proc. 10th Int. Conf. on Nuclear Engineering*, Arlington, VA, USA, Apr. 14–18, 2002, ICONE10-22735, copyright by ASME, (2002).
48) G. H. Su, G. Xiao, Z. Shang, *Applications of Artificial Neural Network and Wavelets in the Reactor Thermal Hydraulic Analysis*, CNIC-01423/XJU-0007, China Nuclear Science and Technology, (1999), [in English].